




Ability of in situ canopy spectroscopy to differentiate genotype by environment interaction in wheat

Arias Claudia, Enrique Montero Bulacio, Rigalli Nicolás, Martín Romagnoli, Facundo Curin, Fernanda G. González, María E. Otegui & Margarita Portapila

To cite this article: Arias Claudia, Enrique Montero Bulacio, Rigalli Nicolás, Martín Romagnoli, Facundo Curin, Fernanda G. González, María E. Otegui & Margarita Portapila (2021) Ability of in situ canopy spectroscopy to differentiate genotype by environment interaction in wheat, *International Journal of Remote Sensing*, 42:10, 3660-3680, DOI: [10.1080/01431161.2021.1875148](https://doi.org/10.1080/01431161.2021.1875148)

To link to this article: <https://doi.org/10.1080/01431161.2021.1875148>

 View supplementary material 

 Published online: 02 Mar 2021.


 Submit your article to this journal 

 View related articles 

 View Crossmark data 



Ability of in situ canopy spectroscopy to differentiate genotype by environment interaction in wheat

Arias Claudia ^a, Enrique Montero Bulacio^a, Rigalli Nicolás^a, Martín Romagnoli^a, Facundo Curin^b, Fernanda G. González^{b,c}, María E. Otegui^d and Margarita Portapila^a

^aCONICET-UNR, Centro Internacional Franco Argentino de Ciencias de la Información y de Sistemas, Universidad Nacional de Rosario, Rosario, Argentina; ^bCITNOBA, CONICET-UNNOBA, Pergamino, Argentina; ^cINTA Estación Experimental Pergamino, Argentina; ^dCONICET-INTA-FAUBA, Estación Experimental Pergamino, Facultad de Agronomía, Universidad de Buenos Aires, Buenos Aires, Argentina

ABSTRACT

In recent years, the application of remote sensing techniques is gaining a growing interest and importance in agriculture. Researchers often combine data from near-infrared and red spectral bands according to their specific objectives. These types of combinations present the disadvantage of lack of sensitivity due to using a single or limited group of bands. In this work on-farm canopy spectral reflectance (CSR) data, composing of ten spectral bands (SBs) plus four spectral vegetation indices (SVIs), is considered in a joint manner to set up a methodology capable to identify genotype by environment interaction (GxE) in wheat. Spectral data are analysed over five wheat genotypes grown in five different environments. Historically breeders have recognized the potentially negative implications of GxE in selection and cultivar deployment and have focused on developing tools and resources to quantify it. We propose to perform a statistical batch processing, applying two-way analysis of variance to multiple spectral data, with genotype and environment as fixed factors. Results prove that this methodology performs well in both directions, capturing differences between genotypes within a single environment, and between environments for a single genotype, representing a step forward to converting spectral data into knowledge for the subject of GxE.

ARTICLE HISTORY

Received 18 June 2020


Accepted 16 December 2020

1. Introduction

In recent years, the application of remote sensing techniques is gaining a growing interest and importance in agriculture. Spectrometers can acquire detailed information regarding the electromagnetic spectrum in a short time, without causing damage and requiring relatively low effort.

Applications of spectral reflectance data for classification purposes are based on the assumption that different spectral responses reproduce differences in biochemical, physiological and structural properties of crops. Such differences are a consequence mainly of

CONTACT Margarita Portapila  portapila@cifasis-conicet.gov.ar  CONICET-UNR, Centro Internacional Franco Argentino de Ciencias de la Información y de Sistemas, Universidad Nacional de Rosario, Rosario, Argentina

 Supplemental data for this article can be accessed [here](#).

© 2021 Informa UK Limited, trading as Taylor & Francis Group

genetics and growing conditions (Cozzolino 2016). Historically breeders have recognized the potentially negative implications of genotype by environment interaction (GxE) in selection and cultivar deployment and have focused on developing tools and resources to quantify it (Cooper et al. 2014; Sadras and Richards 2014). When these interactions exist, they lead to differences and rank changes among genotypes and prevent higher levels of productivity and quality from being achieved. Therefore, the concept of GxE leads to measure the agronomic stability of the genotype over a number of environments. Vargas et al. (2014) point out the importance for researchers of analysing data from experiments to answer questions related to what kind of interaction is there between environments and whether or not there are specific levels of environment effects causing interactions. They considered different treatments, different locations, and different wheat lines. And are particularly interested in strategies for dissecting the interactions, emphasizing that all meaningful interactions that are statistically significant should be reported. Given the mechanistic uncertainty of spectroscopic techniques, more research is needed to develop an efficient methodology to identify GxE.

Wheat is one of the most important cereal species in the human diet worldwide. Due to the population growth, demand for wheat by 2050 is predicted to increase by 70% from today's levels (CIMMYT 2017). Canopy spectral reflectance data (CSR) may provide an objective basis for the macro and micro agricultural management towards a sustainable increase of wheat production. Although CSR is mainly used to correlate with several agronomic traits (Christenson et al. 2014; Ajayi et al. 2016; Garriga et al. 2017; Frels et al. 2017; El-hendawy et al. 2017; Thorp et al. 2017; He et al. 2018; Meacham-Hensold et al. 2019), its capabilities to capture the footprint of different environments on wheat genotypes has not been evaluated. The ability to capture variations in GxE is essential to address cross-cutting issues related to a sustainable wheat production.

The quantitative interpretation of remote-sensing information from vegetation is a complex task. Researchers often combine data from near-infrared and red bands according to their specific objectives. These types of combinations present the disadvantage of lack of sensitivity due to using a single or limited group of bands, particularly evident on heterogeneous canopies (Xue and Su 2017).

Different environments have their variable and complex characteristics, which need to be accounted for when considering CSR information. Different wavebands or spectral vegetation indices (SVIs) have specific suitability and limiting factors. Therefore, for practical applications the choice of spectral data needs to be comprehensive and to combine a set of wavebands and SVIs that span environment diversity.

Thus far, evaluation of CSR in crops and particularly in wheat is done mainly through the analysis of a collection of SVIs, comparing their performance to select a single SVI that better represents a certain trait researchers are interested in (Bort et al. 2005; Gutierrez, Reynolds, and Klatt 2015; Ballester et al. 2017; Zhou et al. 2017; Frels et al. 2017; Maimaitijiang et al. 2020). The potential of analysing spectral bands (SBs) plus SVIs altogether in a batch processing mode had not previously been explored.

The objective of this research is to assess the capabilities of on-farm CSR to identify GxE effects. Ground-based reflectance data were obtained from the wheat canopy of five genotypes grown over five different environments. A statistical batch processing is performed, applying two-way analysis of variance (ANOVA) to multiple spectral data, with genotype and environment as fixed factors. The proposed methodology consists

of a joint analysis of SBs plus SVIs data sets, assessing the commonalities and differences between SBs and SVIs as a whole, capturing differences between genotypes within a single environment, and between environments for a single genotype. The underlying assumption in performing this joint data analysis is that the outcome is more informative than any result obtained by the analysis of each single SB or SVI.

2. Materials and methods

2.1. Study area

Field experiments were conducted in 2017 at two sites: i) Experimental Station of the National Institute of Agricultural Technology (INTA) (33°57'46"S 60°34'25"W) and ii) Experimental plots of the Bioceres Company (33°51'38"S 60°32'21"W), both located in Pergamino, province of Buenos Aires, Argentina. Weather conditions of each site during the growing season of the crops along with soil characteristics are shown in [Table 1](#).

2.2. Plant material and growing conditions

Five wheat (*Triticum aestivum* L.) genotypes ([Table 2](#)) were evaluated under different environmental conditions ([Table 3](#)). Complementary sprinkler irrigation was used in environments E1 and E3, to prevent water deficit mainly during stem elongation and grain filling. Drought conditions in environments E4 and E5 were obtained by covering the plots with rainout shelters when precipitation events occurred since mid of tillering, reaching the plots only 42 mm rain during the growth cycle.

Table 1. Soil characteristics and weather conditions during the growing season.

Variable	INTA	Bioceres
Mean temperature (°C)	14.6	15.0
Mean maximum temperature (°C)	20.0	20.6
Mean minimum temperature (°C)	9.2	9.5
Precipitation (mm)	309.0	326.5
Relative humidity (%)	77.6	76.9
Global solar radiation (Mj m ⁻²)	3025.0	2923.0
Soil type	Typic Argiudoll	Typic Argiudoll
Soil texture	Silty clay loam	Silty clay loam
Nitrogen content (kgN ha ⁻¹)	63.0	ND

Table 2. Wheat genotypes used in the present study.

Name	Acronym	Year of release	Origin	Cycle
Buck Pucará	BP	1980	Argentina	Long
Klein Cacique	KC	1991	Argentina	Long
Klein Pegaso	KP	1997	Argentina	Long
Baguette Premium 11	BP11	2004	Argentina	Long intermediate
Baguette 601	B601	2011	Argentina	Intermediate

Table 3. Crop husbandry of each evaluated environment.

Environment	Acronym	Nitrogen fertilization			Irrigation	
		Rate (kgN ha ⁻¹)	Moments of application	Application form	Water (mm)	Moments of Application
Fertilized – Irrigation	E1 (INTA)	137	DC2.1 and DC3.1	Solid (urea) to the soil	60	DC3.1 to DC9.0
Fertilized – Rainfed	E2 (Bioceres)	200	DC0	Solid (urea + MAP) to the soil	0	–
Unfertilized – Irrigation	E3 (INTA)	0	–	–	60	DC3.1 to DC9.0
Fertilized – Drought	E4 (INTA)	137	DC2.1 and DC3.1	Solid (urea) to the soil	0	–
Unfertilized – Drought	E5 (INTA)	0	–	–	0	–

The experimental design was a randomized complete block with three replications. The genotypes were sown on 1 June at INTA and 26 June at Bioceres in plots of 1.4 m × 5.0 m (7.0 m²) at a density of 280 plants m⁻².

2.3. Spectral reflectance measurements

CSR was measured using a compact shortwave NIR spectrometer (Ocean Insight). The instrument is sensitive to 1024 wavelengths in the range from 632 nm to 1125 nm with an optical resolution at full width half maximum of 3 nm. All measurements were performed between 10:00 and 14:00 hours ART time (UTC – 03:00), with the instrument positioned at a nadir view 50 cm above the surface, thus the diameter of the measured footprint was approximately 26 cm. The upwelling light reflected from a 50 cm × 50 cm white reference material (WRM) with 99% reflectance, was recorded before each canopy measurement allowing data acquisition during variable sky conditions. The dark current was measured through the occlusion of the spectrometer's entrance slot and then subtracted from WRM and canopy measurements. The integration time was adjusted to avoid saturation of the WRM signal and each measurement was the average of five successive scans.

Ten CSRs per plot were measured in the first block at INTA (E1, E3, E4 and E5) and the second block at Bioceres (E2). The measurements were homogeneously distributed over the plot in order to reduce border effects. Plants were measured at different developmental stages for each genotype. Measurements were collected during the three following dates: on 15 September 2017, during the main stem elongation – first node + (14 ± 9) days – ; on 3 November 2017, during grain set/beginning of grain filling – anthesis + (17 ± 8) days – ; and on 9 November 2017, during grain filling/beginning of maturity – anthesis + (24 ± 9) days – . A typical outlier control based on standard deviation was implemented on each CSR raw data.

2.4. Spectral features

To reduce the volume of data and identify influential spectral regions, 10 SBs were defined from the hyperspectral profile. Moreover, selected SVIs were chosen from the literature based on previous work that identified useful applications of these indices for the type of

environments considered in this work. Since the genotype population in this study is morphologically and phenologically diverse – characteristics known to influence the spectral data – we reckon that the strategy of grouping together SBs and SVIs contributes to grasp the interrelationships of crop traits expressing GxE, improving the ability for spectral differentiation.

The SBs are built on combined data from different waveband windows of the spectrum (SB₁ to SB₁₀ in Table 4). Combined bands contain less variation from sample to sample than single-band measurements (Lin, Yang, and Kuo 2012). SB₁ to SB₇ were obtained computing waveband region means, while SB₈ to SB₁₀ were computed as the average gradient of the spectral reflectance curve in a defined window. The selected environment-specific SVIs are: Normalized Difference Vegetation Index (NDVI), Normalized Difference Red Edge (NDRE), Canopy Chlorophyll Content Index (CCCI), and Water Band Index (WBI). The formulas used to evaluate the SBs and the SVIs can be seen in Table 4.

SB₁ and SB₅ are based in 655 nm and 865 nm, respectively, and are necessary to quantitatively evaluate NDVI (Rouse et al. 1974). SB₂ and SB₄ were chosen for being related to the Normalized Difference Red Edge (NDRE), this vegetation index is affected by crop nitrogen status (Herrmann et al. 2010). NDRE is defined based on 720 and 790 nm. SB₁, SB₂, SB₄ and SB₅ are 30 nm wide windows. SB₃ was chosen as a narrowband (3 nm wide, centred in 760 nm) to measure the O₂, a band which is related to Sun-Induced Chlorophyll Fluorescence (SIF). SIF has been applied in different studies to measure vegetation stress (Campbell et al. 2007; Julitta et al. 2016; Mohammed et al. 2019). Since we are interested in wheat nitrogen content in rainfed environments, we included the CCCI (Cammarano et al. 2011) index that is evaluated through SB₁, SB₂, and SB₅. SB₆ and SB₇ were chosen based on the Water Band Index (WBI) (Claudio et al. 2006), centred in 900 nm and 970 nm, respectively, both with a 30 nm wide window. The red-edge region of the spectrum, 680 to 755 nm, is evaluated through its first-order derivative. This interval is divided into three distinct zones to evaluate the average gradient of the curve, resulting in SB₈ (680 to 721 nm), SB₉ (721 to 740 nm) and SB₁₀ (740 to 755 nm). All the spectral data described in this section are summarized in Table 4.

Table 4. Description of the spectral features analysed in this work.

Spectral feature	Wavelength range (nm)	Formula
SB ₁	640 to 670	$SB_i = \frac{1}{n+1} \sum_{j=1}^{n+1} R(\lambda_j),$ <p>where λ is the wavelength value and n is the number of subdivisions of the i spectral wavelength range.</p> $SB_i = \frac{1}{n} \sum_{j=1}^n \frac{R(\lambda_{j+1}) - R(\lambda_j)}{\lambda_{j+1} - \lambda_j}$
SB ₂	705 to 735	
SB ₃	759 to 761	
SB ₄	775 to 805	
SB ₅	850 to 880	
SB ₆	885 to 915	
SB ₇	955 to 985	
SB ₈	680 to 721	
SB ₉	721 to 740	
SB ₁₀	740 to 755	
NDVI		$NDVI = (R_{865} - R_{655}) / (R_{865} + R_{655})$
NDRE		$NDRE = (R_{790} - R_{720}) / (R_{790} + R_{720})$
2*CCCI		$CCCI = \frac{(R_{865} - R_{720}) (R_{865} + R_{655})}{(R_{865} + R_{720}) (R_{865} - R_{655})}$
WBI		$WBI = R_{900} / R_{970}$

2.5. Statistical analysis

In this work we performed a statistical batch processing, applying two-way ANOVA to multiple spectral reflectance data, i.e. the SBs and SVIs listed in Table 4 ('batches' of spectra). Genotype and environment were considered as fixed factors. The ten CSR measurements per plot were considered as replications. Data analysis was conducted in R R18. ANOVA was carried out using the aov-function. The significance of differences was separated using Tukey test at a 5% probability level, using the agricolae-package (de Mendiburu 2020).

3. Results

3.1. Dynamic changes of canopy spectral data

The purpose of this section is to show the variation of the canopy spectral data by genotype for each environment and measurement date. In Figure 1 the red region of the spectrum (SB1) is analysed, in Figure 2 the NIR region (SB2) is considered. A subplot

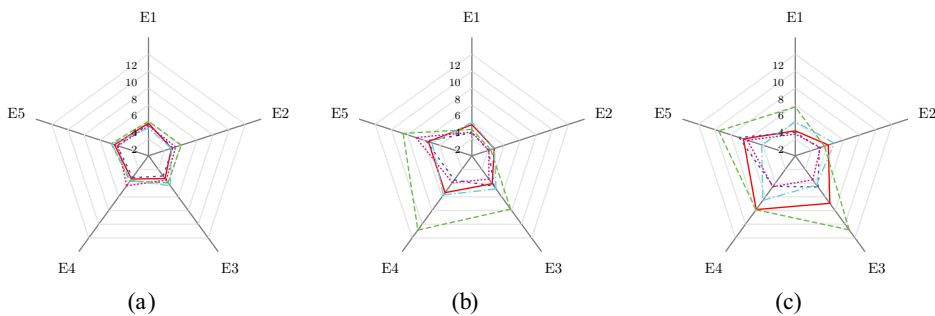


Figure 1. Average reflectance values in percentage at the red region (SB₁) for each genotype and environment at the three measurements days, (a) 15 September 2017, (b) 3 November 2017 and (c) 9 November 2017. B601: Baguette 601 (—), BP11: Baguette Premium 11 (---), KP: Klein Pegaso (...), KC: Klein Cacique(....)and BP: Buck Pucará(.....). (E1: fertilized-irrigation, E2: fertilized-rainfed, E3: unfertilized-irrigation, E4: fertilized-drought and E5: unfertilized-drought).

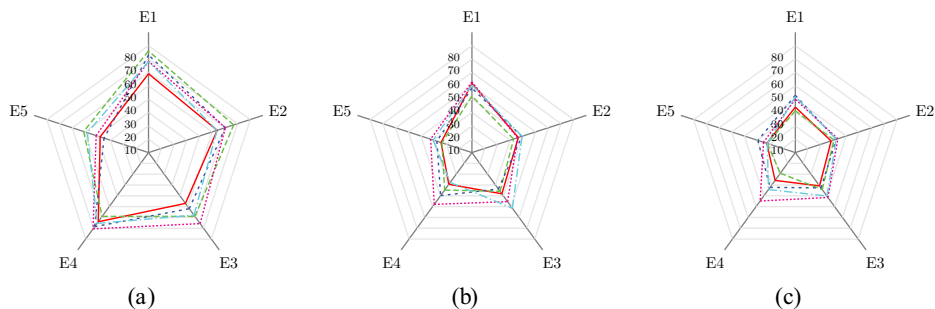


Figure 2. Average reflectance values in percentage at the NIR region (SB₂) for each genotype and environment at the three measurements days, (a) 15 September 2017, (b) 3 November 2017 and (c) 9 November 2017. B601: Baguette 601 (—), BP11: Baguette Premium 11 (---), KP: Klein Pegaso (...), KC: Klein Cacique(....)and BP: Buck Pucará(.....). (E1: fertilized-irrigation, E2: fertilized-rainfed, E3: unfertilized-irrigation, E4: fertilized-drought and E5: unfertilized-drought).

per measurement day is shown. The axis of the subplots displays the average spectral reflectance value for each environment. Different genotypes have been allocated different colours, different axis values per genotype denote the environmental effects. Changes in shape allow us to identify variability between genotypes. To observe the spectral signatures of different genotypes in different environments, graphs by environment and measurement date are provided in the supplemental material (see [Figure 1](#) of the supplemental_material.pdf).

3.2. Environment and genotype performance for reflectance data

To enhance GxE understanding, we propose a joint analysis of SBs plus SVIs. To do this, we perform 48 two-way ANOVA tests (16 spectral features \times 3 measurement days). The 16 spectral features include 10 SBs, 2 SBs ratios (SB_{10}/SB_8 and SB_{10}/SB_9), and 4 SVIs (see [Table 4](#)). These ratios are relations between the spectral bands in the red edge region of the spectrum that we have described and evaluated in previous work (Rigalli et al. 2018). Raw results of the statistical analysis (ANOVA plus Tukey's Honestly Significant Difference) are provided in the supplemental_material_ANOVA.ods file.

As a way to provide a notion of the robustness of the dataset analysed in this work, we estimate the percentage of spectral features that shows significant GxE at three significance levels ($\alpha = 0.050, 0.010$ and 0.001). In [Figure 3](#) these results are plotted for the three measurement days. A bar reaching the value 100% means that the 16 spectral features present significant GxE. Consequently, a higher percentage value implies more spectral features will provide information for the analysis, and therefore a more robust inference will be reached. We can observe in [Figure 3](#) the percentage of features showing significant GxE increases as the crop advances in its cycle. For a significance level of $\alpha = 0.050$, all the spectral features show significant GxE for the second and third measurement day, while the first date reaches 62.5% (10 out of 16 features with $p < 0.050$). For $\alpha = 0.010$, for 3 November 2017 and 9 November 2017, 94% and 100% are respectively reached, while for $\alpha = 0.001$, 81% and 88% are respectively attained. These results meet the requirements of

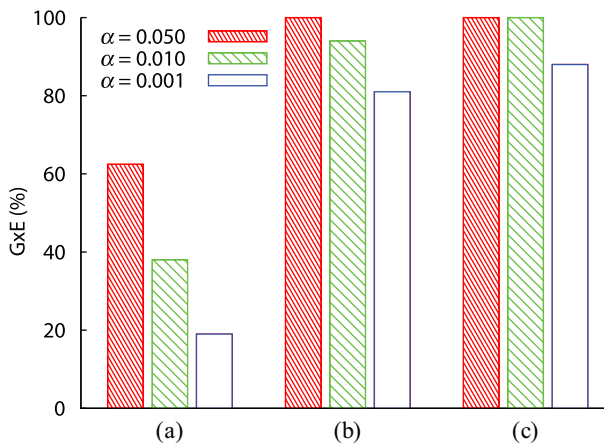


Figure 3. Percentage of spectral features that shows significant GxE ($\alpha = 0.050, 0.010$ and 0.001) for the three measurement days, (a) 15 September 2017, (b) 3 November 2017 and (c) 9 November 2017.

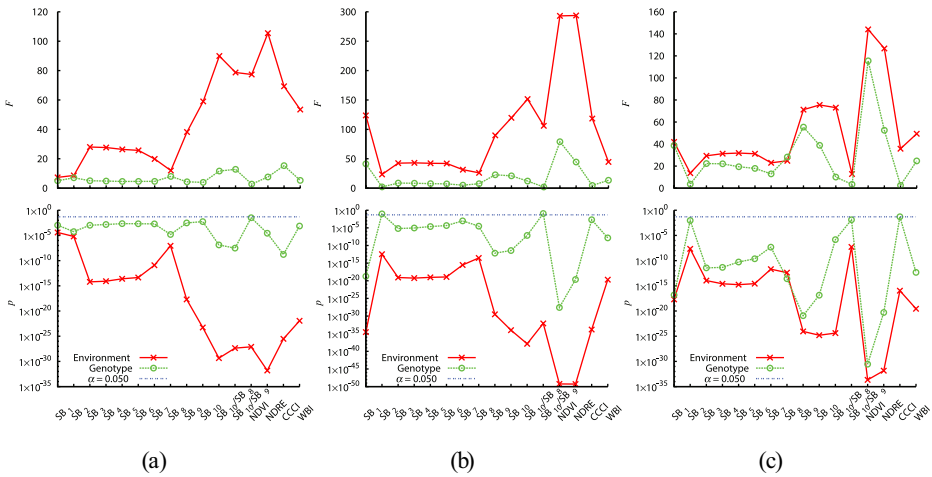


Figure 4. *F*-statistic and *p*-value for environment and genotype factors from each spectral feature’s ANOVA test in the three measurement days, (a) 15 September 2017, (b) 3 November 2017 and (c) 9 November 2017.

dataset robustness and ensure accuracy and consistency of environment and genotype differentiation presented in the following sections.

Once Gx*E* effects were analysed, we will briefly report the statistical behaviour of the independent variables. In **Figure 4** *F*-statistic and *p*-value for environment and genotype are plotted for the three measurement days. In the top row of subplots, we can observe that *F*-values for environment are higher than those for genotype, showing that it is more relevant to the variation between environments than between genotypes. We can establish confidence in these differences since the corresponding *p*-values for both factors are significant, with $p < 0.050$ for the 16 spectral features, and the three dates, with the only two exceptions of SB₂ and SB₁₀/SB₉ for genotype in the second measurement day (see the bottom row of subplots in **Figure 4**, where $\alpha = 0.050$ is represented by a horizontal line; and cells F615 and F1119 in supplemental_material_ANOVA.ods for raw data).

3.3. Environment differentiation

Based on the 48 Tukey’s tests, we obtained 25 results per spectral feature and per day. From these 25 results, made up by the 5 considered genotypes, data were re-arranged per genotype, obtaining blocks like those shown in **Table 5**. The operational procedure that

Table 5. Results of the Tukey’s test, SB₁, 9 November 2017. (BP11: Baguette Premium 11. E1: fertilized-irrigation, E2: fertilized-rainfed, E3: unfertilized-irrigation, E4: fertilized-drought and E5: unfertilized-drought.).

Genotype	Environment	Mean	Standard Deviation	Group
BP11	E3	0.1083	0.0121	a
BP11	E5	0.0950	0.0154	ab
BP11	E4	0.0789	0.0218	bc
BP11	E1	0.0577	0.0155	cdef
BP11	E2	0.0363	0.0051	efg

leads to the identification of the pairs of environments is detailed in the supplemental_material.pdf. In this section we analyse 16 tables (analogous to Table 5), per genotype and measurement day; a total of 240 tables ($16 \times 5 \times 3$). From each table, we identify environment pairs that showed significant differences. For instance, in Table 5 each row corresponds to one environment, to which letters have been assigned as Tukey's results (a, ab, bc, cdef and efg in descending order of mean reflectance values). Therefore, the following environment-pairs can be built: (E1-E5/cdef-ab), (E2-E5/efg-ab) and (E1-E3/cdef-a). Each pair of environments was identified by a number, these codes are detailed in the caption of Table 6 (i.e. 1: E1-E5, 2: E2-E5, 4: E1-E3).

We also identified groups of environments where more than two showed significant differences (three-wise differentiation). Groups of more than two environments were coded by a roman number. In Table 5 fertilized-rainfed (E2, efg), unfertilized-irrigation (E3, a) and fertilized-drought (E4, bc) environments show significant differences (i.e. iv: E2-E3-E4).

This pair-wise/three-wise differentiation of the whole data set (i.e. 240 tables) is summarized in Table 6. Empty cells denote no environment differentiation for the considered spectral feature. Results corresponding to Table 5 (1,2,4,iv) are bolded in Table 6.

As we mentioned before, instead of searching the most sensitive spectral feature, we propose to consider all of them together, in a comprehensive manner. Therefore, the joint contribution of the sixteen spectral features (SBs and SVIs) is determined by adding up data per column in Table 6. All these contributions are summarized in Table 7. The headings of Table 7 are the 10 possible environment pairs that we are willing to differentiate. From left to right we ordered environment-pairs based on the similarities among them. First, contiguous environments (E1-E2, E2-E3, E3-E4 and E4-E5), then, one environment in between (E1-E3, E2-E4 and E3-E5), after that two in-between environments (E1-E4, E2-E5), and finally three environments in between (E1-E5). To illustrate how data from Table 6 are transferred to Table 7 we take the first column in Table 6 (highlighted in grey). This column corresponds to the first measurement day (15 September 2017) and to the Buck Pucara (BP) genotype, where the environment differentiation results are: 1 (E1-E5), 2 (E2-E5), 4 (E1-E3), 5 (E2-E4), 8 (E2-E3), 9 (E3-E4), 10 (E4-E5) and i (E1-E2-E5), which can be disaggregated in 1 (E1-E5), 2 (E2-E5) and 7 (E1-E2). The final list of environment-pairs that could be differentiated is E1-E2, E2-E3, E3-E4, E4-E5, E1-E3, E2-E4, E2-E5, E1-E5 (see the first row of Table 7, highlighted in grey). In consequence, we can state from Table 7 that, on average, 8 out of 10 environment pairs ($119/15 = 7.9$) can be differentiated.

For the first measurement day, on average, 7 out of 10 environment pairs were detected ($8 + 6 + 8 + 7 + 5 = 34/5 = 6.8$). This finding corroborates the possibility of early estimation of the GxE effect. For the second measurement day, 9 out of 10 environment-pairs were differentiated ($7 + 9 + 9 + 9 + 9 = 43/5 = 8.6$), and 8 out of 10 for the third measurement day ($9 + 9 + 8 + 9 + 7 = 42/5 = 8.40$). The difference between E1-E5 and E2-E5 was always detected. E1-E4 was also highly differentiated, except for the first measurement day. These distinctions are likely to happen since we were just differentiating contrasting environments. More challenging would be the capability to identify GxE effects for closer environments. On average, for contiguous environments (E1-E2, E2-E3, E3-E4 and E4-E5) we could differentiate 11 out of 15 cases ($12 + 10 + 10 + 11 = 43/4 =$

Table 6. Environment differentiation. 1: E1-E5, 2: E2-E5, 3: E1-E4, 4: E1-E3, 5: E2-E4, 6: E3-E5, 7: E1-E2, 8: E2-E3, 9: E3-E4, 10: E4-E5. i: E1-E2-E5, ii: E1-E4-E5, iii: E2-E4-E5, iv: E2-E3-E4, v: E1-E3-E4, vi: E1-E2-E4, vii: E1-E3-E5, viii: E2-E3-E5, ix: E1-E2-E3, x: E3-E4-E5. (E1: fertilized-irrigation, E2: fertilized-rainfed, E3: unfertilized-irrigation, E4: fertilized-drought and E5: unfertilized-drought. B601: Baguette 601, BP1: Baguette Premium 11, KP: Klein Pegaso, KC: Klein Cacique and BP: Buck Pucará. Date 1: 15 September 2017, Date 2: 3 November 2017 and Date 3: 9 November 2017.).

SB/SVI	BP			KC			KP			BP11			B601		
	Date 1	Date 2	Date 3	Date 1	Date 2	Date 3	Date 1	Date 2	Date 3	Date 1	Date 2	Date 3	Date 1	Date 2	Date 3
SB ₁	2,8	2,5,7	3	1,2,6,10	1,2	1,2	1	1,2,8	1,2	1,2	ii,iii,iv,v	1,2,4,iv			1,3,4,5,8
SB ₂		8,9	10	2,5,8							5,8	9		2,5	
SB ₃	1	1,3,6,9	1,6,10	1,6,10	1,6,10	1,6,10	1,2,10	1,4	1,3,7	1	1	3,5,9	10	2,3,j	
SB ₄		1,3,6,9	1,6,10	1,6,10	1,6,7,10	1,6,10	1,2,10	1,4	1,3,7	1	1	3,5,9	10	1,3,4,7	
SB ₅		1,3,6,9	1,10,6	1,6,10	1,7,10	1,6,10	1,2,10	1,4	1,3,7	1	1	3,6,9	10	1,3,4,7	
SB ₆		1,3,6,9	1,6,10	1,10	1,7,10	1,6,10	1,10	1,4	1,7	1	1	3,6,9	10	1,3,4,7	
SB ₇		1,3,6,9	1,10,6	1,10	1,7	6,10	1,10	1,4	1,7	1	1	3,6,9	10	1,3,7	
SB ₈	1	3,6,9	1,6,10	8	5,6,8,10	1	1	1	1	1	6	3,5,9	10	1,3,6,7	
SB ₉		1,3,5,6,9	1,3,6,7	6,10,j	1,2,6,10	1,2,10	1,2,10	1,2,10	3,4,i	1	1,2,3,4,5	1,2,3,5,8	10	i,vi,vii	1,2,3,4,5
SB ₁₀	1,4,10	1,2,3,5,6,9	3,6,i	6,i,vii	1,2,6,10	1,2,10	2,8,iv	2,8,iv	1,2,3,4,8	1,2	1,2,3,4,5,8	1,2,3,5,8	1,2,9,10	i,vi,vii	1,2,3,4
SB ₁₀ /SB ₈	1,4,9,10	1,2,3,5,6	1,3,5	1,2,6,10	2,ii,vii	1,10,viii	1,9,iii	1,2,4,8,9,10	1,2,4,8	1,4,5,7,9,10	1,2,3,4,5,8	2,5,8	1,2,9,10	1,2,3,4,5,8	1,2,3,4,5,8
SB ₁₀ /SB ₉	4,9,10,j	1,2	5	4,6,10,j	2,8,10		1,9,10	1,2,4,8,9,10	2,8	4,9,10,j	1,2,3,4,5,8		9,10	1,2,3,4,5,8	
NDVI	1,2,4,8,10	1,2,3,5,6,9	1,3,6,9	1,3,4,7	1,3,4,7	1,3,4,7	1,3,4,7	10,vi,viii	2,ii,vii	1,2,10	iv,v,vi,vii,viii	5,vi,viii	1,2,6,10	1,2,3,5,6,9	i,vi,ix
NDRE	1,4,9,10	1,2,3,5,6,9	1,3,6,9	1,2,6,10	10,vi,viii	1,3,4,7	1,2,x	1,iii,iv	2,8,ii	1,4,5,7,9,10	1,2,3,4,5,8	i,vi,ix	1,2,x	3,5,vii,viii	1,2,3,4,5,8
CCCI	1,4,5,9,10	1,2	1,3,5	1,10	10,vi,viii	1,2	5,9,10	1,2,4,8,9,10	2,4,8	1,5,7,9,10	1,2,3,4,5,8	i,vi,ix	9,10	1,2,4,5,8	1,2,4,8
WBI	1,4	1,3	1,6	1,6	1,3,4,7	1,2	1,3,4,7	1,2	1,2,3	1,2,10	1,2,3	1,2,5	1,2,6,10	1,2,6	1,2,3



Table 7. Contribution of the 16 spectral features to environment differentiation. (E1: fertilized-irrigation, E2: fertilized-rainfed, E3: unfertilized-irrigation, E4: fertilized-drought and E5: unfertilized-drought. B601: Baguette 601, BP11: Baguette Premium 11, KP: Klein Pegaso, KC: Klein Cacique and BP: Buck Pucará. Date 1: 15 September 2017, Date 2: 3 November 2017 and Date 3: 9 November 2017.).

Genotype	Date	Environment differentiation										Number of environment pairs	
		E1-E2	E2-E3	E3-E4	E4-E5	E1-E3	E2-E4	E3-E5	E1-E4	E2-E5	E1-E5		
BP	Date 1	x	x	x	x	x	x	x	x	x	x	x	8
	Date 2	x		x			x	x	x	x	x	x	7
	Date 3	x	x	x			x	x	x	x	x	x	9
KC	Date 1	x			x	x		x	x	x	x	x	6
	Date 2	x	x		x	x		x	x	x	x	x	9
	Date 3	x	x		x	x		x	x	x	x	x	9
KP	Date 1	x			x	x		x	x	x	x	x	8
	Date 2	x	x		x	x		x	x	x	x	x	9
	Date 3	x	x		x	x		x	x	x	x	x	8
BP11	Date 1	x			x	x		x	x	x	x	x	7
	Date 2	x	x		x	x		x	x	x	x	x	9
	Date 3	x	x		x	x		x	x	x	x	x	9
B601	Date 1	x			x	x		x	x	x	x	x	5
	Date 2	x	x		x	x		x	x	x	x	x	9
	Date 3	x	x		x	x		x	x	x	x	x	7
Number of cases the E_i-E_j is differentiated		12	10	10	11	12	12	12	10	15	15	15	119 (119/15 = 7.9)

10.75). In absolute terms 43 out of 60 (72%) cases were successfully discriminated. For those environment-pairs with one in between (E1-E3, E2-E4 and E3-E5), on average we could differentiate 12 out of 15 cases ($12 + 12 + 12 = 36/3 = 12$), and 36 out of 45 (80%) in absolute terms.

3.4. Genotype differentiation

Grain yield and wheat quality are subject to unexpected outcomes from interactions between genotypes and environmental factors (Herrera et al. 2020). The correct application of spectral phenotyping depends on the wheat type and environment (Gizaw, Garland-Campbell, and Carter 2016). Therefore, a robust assessment of the performance of spectral features to differentiate wheat genotypes grown under different environmental conditions is essential. In this section we analysed CSR data in order to discriminate among five genotypes (pair-wise) growing in five environments. This methodology could be used as a proxy to identify the variation in the performance of genotypes in different environments.

Similarly to what we explained in Section 3.3, raw results from Tukey's tests are rearranged, but this time per environment and per measurement day, obtaining blocks like those shown in Table 8. The operational procedure that leads to the identification of the genotypes pairs is detailed in the supplemental_material.pdf. A total of 240 tables (16 spectral features, 5 environments and 3 measurement days) were analysed in this section. From each table, we identified genotype pairs for which a statistically significant difference was found in their CSR data. For instance, in Table 8 each row corresponds to a single genotype, to which letters have been assigned to report Tukey's results, as follows: (KC, abc), (KP, bcde), (BP11, cdef), (B601, ef) and (BP, ef), in descending order of mean reflectance values. Taking this into account we can differentiate Klein Cacique (KC, abc) from Baguette 601 (B601, ef) and Klein Cacique (KC, abc) from Buck Pucará (BP, ef). As it was done for environment-pairs, each pair of genotypes was identified by a number. We also identified three-wise and four-wise combinations of genotypes that were statistically different. Groups of three were coded by lowercase roman numbers, and groups of four were coded by capital roman numbers (for groups coding see Table 9 caption). Information of the pair-wise, three-wise and four-wise differentiations of the whole data set (i.e. 240 tables) is displayed in Table 9. Results corresponding to Table 8 (3: KC-B601, 10: KC-BP) are bolded in Table 9.

The joint contribution of the 16 spectral features (SBs and SVIs) to differentiate genotypes per environment and measurement day was defined by adding up data per column in Table 9. All these contributions are outlined in Table 10. The headings of this

Table 8. Results of the Tukey's test, SB₃, 3 November 2017. (E4: fertilized-drought, B601: Baguette 601, BP11: Baguette Premium 11, KP: Klein Pegaso, KC: Klein Cacique and BP: Buck Pucará.).

Environment	Genotype	Mean	Standard Deviation	Group
E4	KC	0.4020	0.0318	abc
E4	KP	0.3359	0.0564	bcde
E4	BP11	0.2797	0.0233	cdef
E4	B601	0.2368	0.0053	ef
E4	BP	0.2253	0.0478	ef



Table 9. Genotype differentiation. 1: B601-BP, 2: BP11-BP, 3: KC-B601, 4: KP-B601, 5: BP11-KC, 6: KP-BP, 7: BP11-KC, 8: BP11-KP, 9: KC-KP, 10: KC-BP. i: BP11-B601-KC, ii: KC-KP-BP11, iii: KC-KP-B601, iv: KC-KP-BP11, v: KC-BP-BP11, vi: KP-B601-BP11, vii: KP-BP-BP11, viii: BP-B601-BP11. X: KC-BP-B601-BP11. (E1: fertilized-irrigation, E2: fertilized-rainfed, E3: unfertilized-irrigation, E4: fertilized-drought and E5: unfertilized-drought. B601: Baguette 601, BP11: Baguette Premium 11, KP: Klein Pegaso, KC: Klein Cacique and BP: Buck Pucará. Date 1: 15 September 2017, Date 2: 3 November 2017 and Date 3: 9 November 2017.).

2*SB/SVI	E1			E2			E3			E4			E5		
	Date 1	Date 2	Date 3	Date 1	Date 2	Date 3	Date 1	Date 2	Date 3	Date 1	Date 2	Date 3	Date 1	Date 2	Date 3
SB ₁			5,7,8		2,5,7,8	2,8,i		2,5,7,8	3,4,5,8		2,5,7,8	3,4,5,8		2,7,8,10	2,5,7
SB ₂								2,7	2,5						
SB ₃			8		2,6			3,10	2,3,ii						
SB ₄			8		2,6	3		3,10	2,3,ii						
SB ₅			8		2,6			3,10	2,3,ii						
SB ₆			8		2,6			3,10	2,3,5,8,9						
SB ₇					6			10	2,3,5,8						
SB ₈						5		3,10	1,2,3,5,8					5	
SB ₉	5	5	2,4,5,8		2,5,6,9	2,3,5,9		3,4,5,6,8,10	ii,iii,v						
SB ₁₀	7	5	2,5,7,8		2,5,6,9	2,3,5,9		3,4,5,6,8,10	3,8,v						
SB ₁₀ /SB ₈			7		2,5	5		4,5,6,8							
SB ₁₀ /SB ₉										3,9					
NDVI									9						
NDRE			2,5,7,8	6	2,7,ii	4,5,7,8	4,6	6,10,iv	2					5,8,viii	5,8,viii
CCCI					2,5,7,9	3,5,7,8		i,v,vi,vii	4,v	1,3				2,7,8	2,8
WBI			5,7,8		2,5			5,8	2	3,5,9				3	
					6,10	5	2,5	5,10	3,5,9,10	5					

Table 10. Contribution of the 16 spectral features to genotype differentiation. (E1: fertilized-irrigation, E2: fertilized-rainfed, E3: unfertilized-irrigation, E4: fertilized-drought and E5: unfertilized-drought. B601: Baguette 601, BP11: Baguette Premium 11, KP: Klein Pegaso, KC: Klein Cacique and BP: Buck Pucarà. Date 1: 15 September 2017, Date 2: 3 November 2017 and Date 3: 9 November 2017.) The symbol \circ represents new distinguished pairs which are added when the analyses are performed without considering E4 and E5.

Environment	Date	Genotype differentiation													Number of genotype pairs	
		B601-BP11	BP11-KP	KP-KC	KC-BP	B601-KC	KP-BP	B601-KC	BP11-BP	B601-BP	BP11-KP	KP-KC	KC-BP			
E1	Date 1	x														1
	Date 2															1
	Date 3	x	x		\circ	x										5
E2	Date 1		\circ													-
	Date 2															1
	Date 3				\circ	x										3
E3	Date 1				x											3
	Date 2	x	x	x	x	\circ	x	x	x	x	x	x	x	x	x	6
	Date 3	x	x	x	\circ	x	\circ	x	x	x	x	x	x	x	x	7
E4	Date 1			x												3
	Date 2	x	x	x	x	x	x	x	x	x	x	x	x	x	x	8
	Date 3	x	x	x	x	x	x	x	x	x	x	x	x	x	x	9
E5	Date 1															-
	Date 2	x	x		x											7
	Date 3	x	x	x												5
Number of cases the G_j-G_j is differentiated		8	7	4	4	5	5	5	5	7	7	5	5	5	5	59
																(59/15 = 3.9)

table are the 10 possible genotype pairs that we are willing to differentiate. In the absence of a maximum GY-based ranking (the highest-yielding genotype is BP11 for E1, E3, E4, and also for averaged values, but no pattern follows for the rest of the genotypes, as can be seen in Table 11), we defined genotype pairs based on their year of release, as follows: B601-BP11, BP11-KP, KP-KC, KC-BP, B601-KP, BP11-KC, KP-BP, B601-KC, BP11-BP, B601-BP (headers of Table 10 from left to right). As it was done in the previous section, columns of Table 9 were transferred to rows in Table 10. Groups of three or four genotypes (coded in roman numbers) are disaggregated pair-wise. We will illustrate this for column E3/3 November 2017 from Table 9 (highlighted in grey). In this column genotype differentiation results were: 2 (BP11-BP), 5 (BP11-KC), 6 (KP-BP), 7 (BP11-B601), 8 (BP11-KP), 9 (KC-KP), plus ii (KC-KP-BP11), which could be disaggregated in 5 (BP11-KC), 8 (BP11-KP) and 9 (KC-KP). Eventually, the joint contribution from this column was: 2 (BP11-BP), 5 (BP11-KC), 6 (KP-BP), 7 (P11-B601), 8 (BP11-KP), 9 (KC-KP), cross marks highlighted in grey in Table 10. Genotypes grown under limiting factors (drought and/or unfertilized) were more easily discriminated. According to Table 10, E3 (unfertilized-irrigation), E4 (fertilized-drought) and E5 (unfertilized-drought) facilitated genotype differentiation. Regarding measurement days, 15 September 2017 produced poor results, showing that this technique does not perform well for early stages. On the other hand, for the second and third measurement days results corroborate the possibility of genotype discrimination through CSR data. For E4 we could differentiate 17 out of 20 cases (10 genotype-pairs \times 2 dates equals 20), 13 out of 20 for E3 and 12 out of 20 for E5.

4. Discussion

In this section, the discussion is twofold. We compare our work with that of other researchers in the field of remote sensing and we also contrast it with studies on phenotypic data in the ground of GxE, to highlight capacities to address these issues through spectral analysis.

4.1. Environment and genotype differentiation

Regarding the identification of GxE, our results proved that the proposed statistical batch processing performs well at capturing differences between environments for a single genotype. Crossa et al. (2015) claim that it is important to know what the combinations of treatment factors are that cause GxE to draw conclusions with more confidence. In this

Table 11. Grain yield (g m^{-2}) of the wheat genotypes grown in five different environments. (E1: fertilized-irrigation, E2: fertilized-rainfed, E3: unfertilized-irrigation, E4: fertilized-drought and E5: unfertilized-drought. B601: Baguette 601, BP11: Baguette Premium 11, KP: Klein Pegaso, KC: Klein Cacique and BP: Buck Pucará.).

Genotype Environment	BP	KC	KP	BP11	B601	Average
E1	377.20	591.90	669.60	671.10	626.50	587.26
E2	251.95	483.40	590.20	565.50	530.85	484.38
E3	356.70	476.10	454.30	529.95	310.40	425.49
E4	216.42	204.78	217.71	322.87	290.80	250.52
E5	224.88	246.27	240.71	219.46	191.20	224.50
Average	285.43	400.50	434.50	461.78	389.95	394.43

respect, [Table 7](#) shows a very detailed information on the combination of factors that give rise to interactions, since we detect all environment-pairs where interaction occurs.

Unlike other studies, this work analyses spectral reflectance of a variety of environments, where the differences between one and the other are not always extreme. For example, [Garriga et al. \(2017\)](#) evaluate wheat traits by spectral reflectance considering only two contrasting environments (fully and water stress conditions). It should be mentioned that we use a smaller range wavelengths (640 to 985 nm vs 300 to 2500 nm), and a lower cost sensor than in [Garriga et al. \(2017\)](#). Besides, the challenge of discriminating the effects of GxE was much greater, as three additional growing conditions between the two contrasting environments were considered.

[Ajayi et al. \(2016\)](#) and [Garriga et al. \(2017\)](#) analysed the spectral behaviour (300 to 2500 nm) of wheat genotypes under irrigation and water stress conditions. In these reports, the average yield under irrigation was 4 and 3.1 times higher than the average yield under water-stressed conditions, respectively. In the present work, the average yield in an irrigated-fertilized environment (E1) is 2.6 times the average yield in the unfertilized-drought one (E5). This indicates that the contrasting environments considered in this study correspond to growing conditions closer to those reported by the cited authors, which reinforces the results obtained. [Crossa et al. \(2015\)](#) also analysed the phenotypical data to identify the contrasts of the interactions between the environments by evaluating each contrast individually, using a stepwise variable selection to identify the contrasting environments. With our methodology, we can identify interactions in contrasting environments (E1-E5, E2-E5) for all genotypes considered and each measurement date (see [Table 7](#)). Furthermore, the differences between closer growing conditions (fertilized-irrigation from fertilized-rainfed, fertilized-rainfed from unfertilized-irrigation, unfertilized-irrigation from fertilized-drought and fertilized-drought from unfertilized-drought) can be detected with a high degree of accuracy.

Concerning the capability to differentiate genotypes, the methodology performed better on environments with limiting factors (drought and/or unfertilized) than those with optimal growing conditions (fertilized-irrigation and fertilized-rainfed). Unfortunately, there are no remote sensing studies that capture differences between genotypes for a single environment, so it is not possible for us to compare results with previous research. [Garriga et al. \(2017\)](#) used a large set of SVIs for breeding purposes and established two categories of genotypes by taking into account the trait variability range (the lower 80% and the remaining 20%). Even though this dichotomization improved the model performance, it cancels the possibility of capturing differences between two specified genotypes. A similar approach was implemented by [Basati et al. \(2018\)](#), considering only two main classes of healthy and unhealthy genotypes for detecting sunn pest damaged wheat samples after an unsuccessful attempt of identifying among five different classes.

Additionally, we can determine which of the five genotypes is more susceptible to be segregated from the others. On the third measurement date, BP11 is differentiated from other genotypes 16 out of 20 times, and B601 is distinguished from the others 13 out of 20 times. On the second measurement date, BP11 is distinguishable from other genotypes 13 out of 20 times, when KC and BP are differentiated 9 out of 20 times. Whereas for the first date, BP11, B601, KC, and BP are only differentiated 3 out of 20 times. For genotype pairs

and environments in which genotypes can be differentiated, see [Figure 4](#) of the supplemental_material.pdf.

4.2. Genotype differentiation performance on productive environments

Since drought stress is the most severe environmental stress for plant growth and crop production we were also interested in assessing the CSR capability for genotype differentiation under favourable environments. By performing two-way ANOVA on E1, E2 and E3 only, we removed spectral variability due to drought stress. Taking out E4 and E5 from the variance analysis, seven additional genotype-pairs could be differentiated (circles in [Table 10](#)). Two corresponded to the second measurement day: BP11-KP for E2 and B601-KP for E3; and five to the third measurement day: KC-BP for E1, KC-BP and BP11-KC for E2 and KC-BP and KP-BP for E3. As mentioned for the full analysis, i.e. considering the five environments, better performance was obtained for measurements taken at post-anthesis stages (grain set/beginning of grain filling for the second and grain filling/beginning of maturity for the third measurement day). These results are in concordance with [Frels et al. \(2017\)](#) and [Prey, Hu, and Schmidhalter \(2020\)](#), who found that grain filling is the most suitable phase for their analysed traits.

4.3. Spectral features sensitivity

Results in [Table 6](#) and [Table 9](#) provide statistical support for environment and genotype differentiation in the context of GxE. From spectral features sensitivity, we can recognize patterns. SBs performance at the NIR-plateau (between 759 nm and 915 nm, i.e. SB₃, SB₄, SB₅, SB₆) are similar, as it is also reported in [Prey, Hu, and Schmidhalter \(2020\)](#). Red Edge-SBs (between 721 nm and 755 nm, i.e. SB₉ and SB₁₀) present a high sensitivity providing additional pair-wise discrimination, for both environments and genotypes, detecting differences that can not be captured at the NIR-plateau wavebands. The usefulness of red edge bands can be attributed to increased sensitivities in dense canopies ([Prey, Hu, and Schmidhalter 2020](#)). Besides, the SB in the red region (SB₁), adds up pair-wise differentiations that are not captured by other SBs nor SVIs. On this regard, [Ajayi et al. \(2016\)](#) reported differences in reflectance values at the red region among genotypes under irrigated conditions. Finally, SVIs also contribute to differentiate pairs that are not identified by any SB, performing better for environment differentiation (for what they have been developed) than for genotype differentiation. Still, they play a part for genotype distinction.

While the results are unable to elucidate a key mechanistic understanding of what this spectral method is measuring, they are not simply a proxy for detection of GxE since this methodology can be very useful in phenotyping wheat varieties. This joint analysis of SBs plus SVIs data sets considers crops and environment as a complete system, where spectral data detect information in a holistic manner.

We consider that using established reflectance-based approaches, particularly related to single SVIs, would limit their capacity and may not apply for GxE identification. GxE is foundational to understanding the genetic basis of trait variation, but still, hypotheses explaining this variation remain fragmented ([Saltz et al. 2018](#)). We understand that the

proposed methodology broadens the applicability of spectral data and vegetation indices all together.

Although the proposed methodology is purely empirical, its robustness is linked to the use of SBs and SVIs widely used in remote sensing applications. Additionally, we consider three consecutive segments of the spectrum 680 to 721 nm, 721 to 740 nm and 740 to 755 nm, where we compute the average gradient of the curve, SB_8 , SB_9 and SB_{10} , respectively. These three spectral features represent the variability pattern of the red-edge band of the spectrum. The spectral curve shape has seldom been used because it is difficult to be quantified. Therefore, for the replicability of this method, it is necessary to collect data with a field spectrometer, and not just with a red-green-blue-NIR sensor to be able to evaluate SB_8 , SB_9 and SB_{10} .

5. Conclusions

The results obtained in this work offer an effective approach to leverage CSR data that is increasingly being collected in agriculture. With a limited rank of spectral features, collected with a low-cost field spectrometer and a few vegetation indices, researchers can generate a spectral dataset with high capabilities to identify GxE. The innovation we present is that we perform a statistical batch processing, applying two-way ANOVA to multiple spectral reflectance data, what we call batches of spectra, assessing the results as a whole. In this way, we get a deeper insight into the GxE. A joint analysis of SBs plus SVIs data sets proves capable of discrimination between environments as well as capable of differentiating wheat genotypes. We can ensure a fair contribution by the different spectral features considered in the analysis since all pair-wise differentiation is based on statistically significant results.

This methodology offers the potential of payoff in terms of distinctiveness, uniformity and stability testing (procedures needed in Europe for new varieties, apart from grain yield itself), opening current bottlenecks to crop improvement. Complex interactions between genotypes and environments determine the development of plants, but their separate contribution to the phenotype remains unclear. If complex interactions can be identified, this is a first step for studying and interpreting the reasons and circumstances of these effects completely and correctly. And doing so by a remote sensing technique will accelerate the replication of the analyses. We believe that the methodology developed in this work can help minimize the confounding effects, identifying subtle differences between cultivars within a single environment, and the effects of different environments on a certain cultivar, representing a step forward to converting spectral data into knowledge.

The imperative to breed crops into harsher environments demands a better understanding of adaptation, as a consequence innovative remote sensing technologies will play a fundamental role in breeding processes. Remotely sensed data for plant phenotyping have reached such a level that we can raise the question of whether data-driven approaches can replace traditional hypothesis-driven analyses. Results reached in this work may indeed provide us with new insights into GxE in wheat, a methodology that can be extended to other staple crops.

Besides, the need to understand the agronomic ecosystem functioning over large spatial scales may lead to implement this approach through unmanned aerial vehicles,

increasing the screening capabilities by orders of magnitude and provide critical information on canopy-scale GxE in real-time. Furthermore, using this type of CSR methodologies can lead to more robust decision-making tools regarding land use/land cover scenarios.

Disclosure statement

No potential conflict of interest was reported by the authors.

Funding

This work was supported by Agencia Nacional de Promoción Científica y Tecnológica, PICT 2015 2671.

ORCID

Arias Claudia  <http://orcid.org/0000-0003-3345-030X>

Data availability statement

The authors confirm that the data supporting the findings of this study are available within the article and its supplemental material.

References

- Ajayi, S., S. K. Reddy, P. H. Gowda, Q. Xue, J. C. Rudd, G. Pradhan, S. Liu, B. A. Stewart, C. Biradar, and K. E. Jessup. 2016. "Spectral Reflectance Models for Characterizing Winter Wheat Genotypes." *Journal of Crop Improvement* 30 (2): 176–195. doi:10.1080/15427528.2016.1138421.
- Ballester, C., J. Hornbuckle, J. Brinkhoff, J. Smith, and W. Quayle. 2017. "Assessment of In-season Cotton Nitrogen Status and Lint Yield Prediction from Unmanned Aerial System Imagery." *Remote Sensing* 9 (11): 1149. doi:10.3390/rs9111149.
- Basati, Z., B. Jamshidi, M. Rasekh, and Y. Abbaspour-Gilandeh. 2018. "Detection of Sunn Pest-damaged Wheat Samples Using Visible/near-infrared Spectroscopy Based on Pattern Recognition." *Spectrochimica Acta. Part A, Molecular and Biomolecular Spectroscopy* 203: 308–314. doi:10.1016/j.saa.2018.05.123.
- Bort, J., J. Casadesus, M. M. Nachit, and J. L. Araus. 2005. "Factors Affecting the Grain Yield Predicting Attributes of Spectral Reflectance Indices in Durum Wheat: Growing Conditions, Genotype Variability and Date of Measurement." *International Journal of Remote Sensing* 26 (11): 2337–2358. doi:10.1080/01431160512331337808.
- Cammarano, D., G. Fitzgerald, B. Basso, G. O'Leary, D. Chen, P. Grace, and C. Fiorentino. 2011. "Use of the Canopy Chlorophyll Content Index (CCCI) for Remote Estimation of Wheat Nitrogen Content in Rainfed Environments." *Agronomy Journal* 103: 1597–1603. doi:10.2134/agronj2011.0124.
- Campbell, P. K. E., E. M. Middleton, J. E. McMurtrey, L. A. Corp, and E. W. Chappelle. 2007. "Assessment of Vegetation Stress Using Reflectance or Fluorescence Measurements." *Journal of Environmental Quality* 36 (3): 832–845. doi:10.2134/jeq2005.0396.
- Christenson, B. S., W. T. Schapaugh, N. An, K. P. Price, and A. K. Fritz. 2014. "Characterizing Changes in Soybean Spectral Response Curves with Breeding Advancements." *Crop Science* 54 (4): 1585–1597. doi:10.2135/cropsci2013.08.0575.
- CIMMYT. 2017. "New Publications: Improving Wheat Breeding through Modern Genetic Tools." <https://www.cimmyt.org/publications/new-publications-improving-wheat-breeding-through-modern-genetic-tools/>

- Claudio, H. C., Y. Cheng, D. A. Fuentes, J. A. Gamon, H. Luo, W. Oechel, H. Qiu, A. F. Rahman, and D. A. Sims. 2006. "Monitoring Drought Effects on Vegetation Water Content and Fluxes in Chaparral with the 970 Nm Water Band Index." *Remote Sensing of the Environment* 103 (3): 304–311. doi:10.1016/j.rse.2005.07.015.
- Cooper, M., C. D. Messina, D. Podlich, L. R. Totir, A. Baumgarten, N. J. Hausmann, D. Wright, and G. Graham. 2014. "Predicting the Future of Plant Breeding: Complementing Empirical Evaluation with Genetic Prediction." *Crop & Pasture Science* 65 (4): 311–336. doi:10.1071/CP14007.
- Cozzolino, D. 2016. "Authentication of Cereals and Cereal Products." *Advances in Food Authenticity Testing* 136: 441–457.
- Crossa, J., M. Vargas, C. M. Cossani, G. Alvarado, J. Burgueño, K. L. Mathews, and M. P. Reynolds. 2015. "Evaluation and Interpretation of Interactions." *Agronomy Journal* 107 (2): 736–747. doi:10.2134/agronj2012.0491.
- de Mendiburu, F. 2020. *Statistical Procedures for Agricultural Research*. Vienna, Austria: R Foundation for Statistical Computing. <http://www.R-project.org/>
- El-hendawy, S., W. Hassan, N. Al-suhaibani, and U. Schmidhalter. 2017. "Spectral Assessment of Drought Tolerance Indices and Grain Yield in Advanced Spring Wheat Lines Grown under Full and Limited Water Irrigation." *Agricultural Water Management* 217: 82–92.
- Frels, K., M. Guttieri, B. Joyce, B. Leavitt, and P. Baenziger. 2017. "Evaluating Canopy Spectral Reflectance Vegetation Indices to Estimate Nitrogen Use Traits in Hard Winter Wheat." *Field Crop Research* 217: 1–12.
- Garriga, M., S. Romero-Bravo, F. Estrada, A. Escobar, I. A. Matus, A. Del Pozo, C. A. Astudillo, and G. A. Lobos. 2017. "Assessing Wheat Traits by Spectral Reflectance: Do We Really Need to Focus on Predicted Trait-Values or Directly Identify the Elite Genotypes Group?" *Frontiers in Plant Sciences* 8: 280.
- Gizaw, S. A., K. Garland-Campbell, and A. H. Carter. 2016. "Use of Spectral Reflectance for Indirect Selection of Yield Potential and Stability in Pacific Northwest Winter Wheat." *Field Crop Research* 196: 199–206. doi:10.1016/j.fcr.2016.06.022.
- Gutierrez, M., P. Reynolds, and A. R. Klatt. 2015. "Effect of Leaf and Spike Morphological Traits on the Relationship between Spectral Reflectance Indices and Yield in Wheat." *International Journal of Remote Sensing* 36 (3): 701–718. doi:10.1080/01431161.2014.999878.
- He, R., H. Li, X. Qiao, and J. Jiang. 2018. "Using Wavelet Analysis of Hyperspectral Remote-sensing Data to Estimate Canopy Chlorophyll Content of Winter Wheat under Stripe Rust Stress." *International Journal of Remote Sensing* 39 (12): 4059–4076. doi:10.1080/01431161.2018.1454620.
- Herrera, J. M., L. L. Häner, F. Mascher, J. Hiltbrunner, D. Fossati, C. Brabant, R. Charles, and D. Pellet. 2020. "Lessons from 20 Years of Studies of Wheat Genotypes in Multiple Environments and under Contrasting Production Systems." *Frontiers in Plant Science* 10: 1745. doi:10.3389/fpls.2019.01745.
- Herrmann, I., A. Karnieli, D. J. Bonfil, Y. Cohen, and V. Alchanatis. 2010. "Swir-based Spectral Indices for Assessing Nitrogen Content in Potato Fields." *International Journal of Remote Sensing* 31 (19): 5127–5143. doi:10.1080/01431160903283892.
- Julitta, T., L. A. Corp, M. Rossini, A. Burkart, S. Cogliati, N. Davies, M. Hom et al.. 2016. "Comparison of Sun-Induced Chlorophyll Fluorescence Estimates Obtained from Four Portable Field Spectroradiometers." *Remote Sensing* 8 (2): 2. DOI:10.3390/rs8020122.
- Lin, W. S., C. M. Yang, and B. J. Kuo. 2012. "Classifying Cultivars of Rice (*Oryza Sativa* L.) Based on Corrected Canopy Reflectance Spectra Data Using the Orthogonal Projections to Latent Structures (O-PLS) Method." *Chemometrics and Intelligent Laboratory Systems* 115: 25–36. doi:10.1016/j.chemolab.2012.04.005.
- Maimaitijiang, M., V. Sagan, P. Sidike, S. Hartling, F. Esposito, and F. B. Fritschi. 2020. "Soybean Yield Prediction from UAV Using Multimodal Data Fusion and Deep Learning." *Remote Sensing of Environment*, 237. <https://doi.org/10.1016/j.rse.2019.111599>
- Meacham-Hensold, K., C. M. Montes, J. Wu, K. Guan, P. Fu, E. A. Ainsworth, T. Pederson, et al.. 2019. "High-throughput Field Phenotyping Using Hyperspectral Reflectance and Partial Least Squares Regression (PLSR) Reveals Genetic Modifications to Photosynthetic Capacity." *Remote Sensing of Environment* 231: 231. doi:10.1016/j.rse.2019.04.029.

- Mohammed, G. H., R. Colombo, E. M. Middleton, U. Rascher, C. van der Tol, L. Nedbal, Y. Goulas et al. 2019. "Remote Sensing of Solar-induced Chlorophyll Fluorescence (SIF) in Vegetation: 50 Years of Progress." *Remote Sensing of Environment*, 231. <https://doi.org/10.1016/j.rse.2019.04.030>
- Prey, L., Y. Hu, and U. Schmidhalter. 2020. "High-throughput Field Phenotyping Traits of Grain Yield Formation and Nitrogen Use Efficiency: Optimizing the Selection of Vegetation Indices and Growth Stages." *Frontiers in Plant Science* 10: 1672. doi:10.3389/fpls.2019.01672.
- R Core Team. 2018. *R: A Language and Environment for Statistical Computing*. Vienna, Austria: R Foundation for Statistical Computing. <http://www.R-project.org/>
- Rigalli, N. F., E. M. Bulacio, M. Romagnoli, L. Terissi, and M. Portapila. 2018. "Identification and Characterization of Crops through the Analysis of Spectral Data with Machine Learning Algorithms." *Argentinian Conference of Information Technology* 374–387. <http://47jaiio.sadio.org.ar/sites/default/files/CAI-50.pdf>
- Rouse, J. W., R. H. Haas, J. A. Schell, D. W. Deering, and J. C. Harlan. 1974. "Monitoring the Vernal Advancement and Retrogradation of Natural Vegetation." *Technical Report*. <https://ntrs.nasa.gov/search.jsp?R=19740022555>
- Sadras, V. O., and R. A. Richards. 2014. "Improvement of Crop Yield in Dry Environments: Benchmarks, Levels of Organisation and the Role of Nitrogen." *Journal of Experimental Botany*. doi:10.1093/jxb/eru061.
- Saltz, J. B., A. M. Bell, J. Flint, R. Gomulkiewicz, K. A. Hughes, and J. Keagy. 2018. "Why Does the Magnitude of Genotype-by-environment Interaction Vary?." *Ecology and Evolution* 8 (12): 6342–6353. doi:10.1002/ece3.4128.
- Thorp, K., G. Wang, K. Bronson, M. Badaruddin, and J. Mon. 2017. "Hyperspectral Data Mining to Identify Relevant Canopy Spectral Features for Estimating Durum Wheat Growth, Nitrogen Status, and Grain Yield." *Computers and Electronics in Agriculture* 136: 1–12. doi:10.1016/j.compag.2017.02.024.
- Vargas, M., B. Glaz, G. Alvarada, J. Pietragalla, A. Morgounov, Y. Zelenskiy, and J. Crossa. 2014. "Analysis and Interpretation of Interactions in Agricultural Research." *Agronomy Journal* 107 (2): 748–762. doi:10.2134/agronj13.0405.
- Xue, J., and B. Su. 2017. "Significant Remote Sensing Vegetation Indices: A Review of Developments and Applications." *Journal of Sensors* 2017: 1–17. doi:10.1155/2017/1353691.
- Zhou, X., H. Zheng, X. Xu, J. He, X. Ge, X. Yao, T. Cheng, Y. Zhu, W. Cao, and Y. Tian. 2017. "Predicting Grain Yield in Rice Using Multi-temporal Vegetation Indices from UAV-based Multispectral and Digital Imagery." *ISPRS Journal of Photogrammetry and Remote Sensing* 130: 246–255. doi:10.1016/j.isprsjprs.2017.05.003.